

Do Language Models Plan for Future Tokens?

Wilson Wu
Department of Mathematics
University of Colorado Boulder
wiwu2390@colorado.edu

John X. Morris
Department of Computer Science
Cornell University
jxm3@cornell.edu

Lionel Levine
Department of Mathematics
Cornell University
levine@math.cornell.edu

Abstract

Do transformers “think ahead” during inference at a given position? It is known transformers prepare information in the hidden states of the forward pass at t that is then used in future forward passes $t + \tau$. We posit two explanations for this phenomenon: *pre-caching*, in which off-diagonal gradient terms present in training result in the model computing features at t irrelevant to the present inference task but useful for the future, and *breadcrumbs*, in which features most relevant to time step t are already the same as those that would most benefit inference at time $t + \tau$. We test these hypotheses by training language models without propagating gradients to past timesteps, a scheme we formalize as *myopic training*. In a synthetic data setting, we find clear evidence for pre-caching. In the autoregressive language modeling setting, our experiments are more suggestive of the breadcrumbs hypothesis.

1 Introduction

Humans are known to think ahead while speaking; decades of linguistics research (Huetting, 2015; Miller, 1951) have shown evidence that human language users internally predict upcoming language input, words and sometimes sentences ahead (Barthel et al., 2016).

Unlike humans, contemporary language models allocate a fixed amount of information processing for each token when “speaking” (Vaswani et al., 2017). Do language models, like humans, think ahead? Recent work (Pal et al., 2023; Hernandez et al., 2024; Cai et al., 2024) has shown that tokens beyond the immediate next token can be predicted by probing the hidden state of the language model. Intriguingly, model outputs at future tokens can be predicted to some extent using linear probes on model hidden states, and interventions on hidden states can predictably alter future outputs.

These findings indicate that model activations at a given timestep are at least somewhat predictive of future outputs. However, it remains unclear why this might be: is this just a happenstance property of the data, or because the model is deliberately preparing information for future timesteps, at the expense of degrading performance on the current position?

We observe that gradients during training optimize weights for both the loss at the current token position as well as for tokens later in the sequence. We question to what extent current transformer weights dedicate resources to the current token vs. allocating it for future tokens.

We consider two possibilities: the *pre-caching* hypothesis, in which the transformer learns to compute features at time step t that are irrelevant to the inference task at that current time step but may be useful for future time steps $t + \tau$, and the *breadcrumbs* hypothesis, in

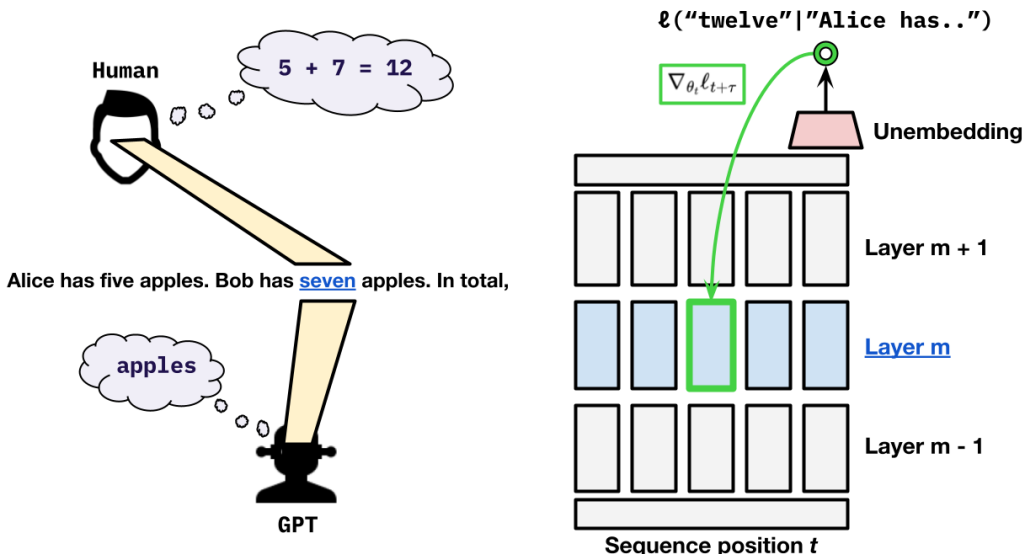


Figure 1: At which position is the computation required to correctly answer this math problem taking place? Cognitive science tells us that humans think ahead while speaking, while our evidence suggests that LLMs do not do so to the same extent.

which the features most relevant to time step t are already identical to those that would most benefit inference at time $t + \tau$. To evaluate which hypothesis might be correct, we propose a *myopic* training scheme which does not propagate gradients from the loss at the current position to hidden states from previous positions.

To consider whether language models might directly implement pre-caching, we design a synthetic scenario where the task can only be completed via explicit pre-caching. We configure a task where the model must precompute information for the next token, because otherwise the correct answer could not be accurately computed in a single forward pass. In this synthetic scenario, we find clear evidence that the transformer learns to pre-cache. When transformer-based sequence models must precompute information to minimize loss, they do so.

We then consider whether breadcrumbs or pre-caching is demonstrated in natural language models (pre-trained GPT-2 variants). Our experiments with myopic training suggest that much less pre-caching occurs in this setting, and thus point towards the breadcrumbs hypothesis.

On real language data, we claim language models do not intentionally prepare information for the future to a significant extent. Instead, they compute features that are useful to predicting the immediate next token, which turn out to then be helpful at future steps. In language data, we do not observe a significant tradeoff between greedily optimizing for next token loss and ensuring future predictive performance.

2 Related work

Future token meta-prediction. Several recent works (nostalgebraist, 2020; Belrose et al., 2023; Pal et al., 2023; Cai et al., 2024) observe that transformer hidden states can be used to predict current and future tokens in a sequence, typically via linear probing. Notably, Hernandez et al. (2024) show that more complicated relationships are encoded linearly in hidden states, such as subject-object relations, implying that future tokens can also be predicted in specific cases. Unlike these works, we consider whether the model is deliberately preparing hidden states that are useful for future prediction, at the expense of current-token predictivity.

Probing. Our experiments make use of *probing*, a technique where a simple auxiliary model is used to predict properties from target models’ representations (Belinkov & Glass, 2019; Shi et al., 2016; Hewitt & Liang, 2019; Pimentel et al., 2020; Belinkov, 2021). We can also phrase our probing experiments as measuring the \mathcal{V} -information contained in a representation vector, where \mathcal{V} is the class of linear models (Xu et al., 2020; Hewitt & Liang, 2019). Probing-based approaches are known to overestimate latent information if the classifier learns to do a task on its own (Belinkov, 2021), and probing analyses may only be informative when compared to probing a reasonable baseline (Hewitt & Liang, 2019). In our probing experiments, we avoid these pitfalls by ensuring that the function to be learned cannot possibly be computed by the probe itself.

Mechanistic interpretability. Our analysis of transformer models in a synthetic setting relates to the subfield of *mechanistic interpretability*, which seeks to understand models by isolating and explaining the behavior of their components (Olah et al., 2020; Bau et al., 2020; Meng et al., 2023; Nanda et al., 2023). Some of these works (Nanda et al., 2023; Li et al., 2023; Zhong et al., 2023) practice mechanistic interpretability by studying models trained on synthetic worlds. We apply some mechanistic interpretability techniques in a synthetic setting to study the problem of whether language models “think ahead” for future tokens.

3 Theory: Pre-caching or breadcrumbs?

Consider a generic causal sequence-to-sequence prediction task

$$(\mathbf{x}_1, \dots, \mathbf{x}_n, \mathbf{y}_1, \dots, \mathbf{y}_n) \sim \mathcal{D},$$

where \mathcal{D} is a data distribution supported on $\mathbb{X}^n \times \mathbb{Y}^n$ for some domains \mathbb{X}, \mathbb{Y} . The task is to estimate the conditional expectations $\mathbb{E}_{\mathcal{D}}(\mathbf{y}_i \mid \mathbf{x}_1, \dots, \mathbf{x}_i)$ for $1 \leq i \leq n$.¹ Note that we recover the autoregressive setting by setting $\mathbb{Y} = \mathbb{X}$ and $\mathbf{y}_i := \mathbf{x}_{i+1}$.

Transformer models trained on such tasks have been observed (Pal et al., 2023) to store information in hidden states during inference at position i that is then used in future inference at $j > i$. However, since the loss associated with each step i depends only on how well the model does at the immediate task of predicting \mathbf{y}_i , it is not immediately clear how this preparation for the future arises. We give names to two competing explanations:

- **Pre-caching:** The model “deliberately” computes and stores features that are expected to be useful for the future, even if they are irrelevant to the present.
- **Breadcrumbs:** The features that most benefit the present inference task are the same as those that are most useful to the future. When the model performs the present forward pass, it “unintentionally” leaves a trace (“breadcrumbs”) that is then picked up by future passes.

To disentangle these two explanations, we introduce a notion of *myopic* transformer models, which we show to be incapable of deliberate pre-caching—for these models, the extent to which past features are beneficial to the future is decided purely by the breadcrumbs explanation. Thus, the gap between vanilla and myopic transformer models is a quantitative measure of how much pre-caching is taking place.

3.1 Transformer preliminaries

Suppose, for the sake of exposition, that the transformer model G uses independent parameters for each position $1, \dots, n$.² Let p be the parameter count of each forward pass of G . Then, letting $\theta_i \in \Theta = \mathbb{R}^p$ be all parameters used by G at position i , a transformer G is a parameterized function

$$G: \mathbb{X}^n \times \Theta^n \rightarrow \mathbb{Y}^n, \quad (\mathbf{x}_1, \dots, \mathbf{x}_n; \theta_1, \dots, \theta_n) \mapsto (\hat{\mathbf{y}}_1, \dots, \hat{\mathbf{y}}_n).$$

¹For classification tasks, we are typically interested in the conditional probabilities $\Pr_{\mathcal{D}}(\mathbf{y}_n = c \mid \mathbf{x}_1, \dots, \mathbf{x}_n)$ for each class c . However, this can be subsumed into the generic case by letting \mathbb{Y} be the probability simplex over all classes.

²For example, this is true of absolute position embedding weights.

For $1 \leq i \leq n$, let $G_i(\mathbf{x}_1, \dots, \mathbf{x}_n) \in \mathbb{Y}$ be the output of G 's i th forward pass. Because of the causal masking within G , this depends only on $\mathbf{x}_1, \dots, \mathbf{x}_i$ and $\theta_1, \dots, \theta_i$. That is, with slight abuse of notation, we may write

$$\hat{\mathbf{y}}_i = G_i(\mathbf{x}_1, \dots, \mathbf{x}_n; \theta_1, \dots, \theta_n) = G_i(\mathbf{x}_1, \dots, \mathbf{x}_i; \theta_1, \dots, \theta_i).$$

3.2 Off-diagonal gradient terms

Now, letting $\mathcal{L}: \mathbb{Y} \times \mathbb{Y} \rightarrow \mathbb{R}_+$ be some choice of loss function, the expected loss ℓ of a transformer model with parameters $\theta_1, \dots, \theta_n$ is

$$\ell(\theta_1, \dots, \theta_n) := \mathbb{E}_{(\bar{\mathbf{x}}, \bar{\mathbf{y}}) \sim \mathcal{D}} \sum_{i=1}^n \mathcal{L}(G_i(\mathbf{x}_1, \dots, \mathbf{x}_i; \theta_1, \dots, \theta_i), \mathbf{y}_i) =: \sum_{i=1}^n \ell_i(\theta_1, \dots, \theta_i),$$

the sum over $1 \leq i \leq n$ of the expected loss ℓ_i at position i . (We suppress the dependence on G and \mathcal{D} for concision.) In practice, we always tie the weights across position. That is, all θ_i are set equal to the same $\theta \in \Theta$. Then, by the chain rule,

$$\nabla_{\theta} \ell(\theta, \dots, \theta) = \sum_{i=1}^n \nabla_{\theta_i} \ell(\theta_1, \dots, \theta_n) \Big|_{\theta_1 = \dots = \theta_n = \theta} = \sum_{i=1}^n \sum_{j=i}^n \nabla_{\theta_i} \ell_j(\theta_1, \dots, \theta_j) \Big|_{\theta_1 = \dots = \theta_n = \theta},$$

a sum over an upper-triangular expected Jacobian ‘‘matrix’’. The off-diagonal terms $i < j$, corresponding to the expected gradient of the model’s future loss at position j wrt. its weights at position i , are the training signals that encourage pre-caching.

3.3 Measuring pre-caching: The myopia gap

We say a model is *myopic* when each forward pass G_i optimizes only ℓ_i without regard for future ℓ_j at $j > i$. In the untied weights case, the right definition is then apparent.

Definition 1. The parameters $\tilde{\theta}_1, \dots, \tilde{\theta}_n$ are *untied-myopic* if they satisfy

$$\tilde{\theta}_i \in \arg \min_{\theta_i} \ell_i(\tilde{\theta}_1, \dots, \tilde{\theta}_{i-1}, \theta_i) \quad \forall i \in \{1, \dots, n\}. \quad (1)$$

Definition 2. Let \mathbb{M} be the feasible set of the constraints in Equation 1. The *untied myopia gap* is the smallest possible gap between the expected loss attained by a myopic model and the optimal model:

$$p^* := \min_{\tilde{\theta}_1, \dots, \tilde{\theta}_n \in \mathbb{M}} \ell(\tilde{\theta}_1, \dots, \tilde{\theta}_n) - \min_{\theta_1, \dots, \theta_n} \ell(\theta_1, \dots, \theta_n). \quad (2)$$

In the tied weights case, it is perhaps not immediately clear what the right definition of myopia should be. It does not suffice to simply constrain the minimizations in Equation 1 to $\tilde{\theta}_1 = \dots = \tilde{\theta}_n$, since $\min_{\theta} \ell_i(\theta, \dots, \theta)$ is optimizing for pre-caching (the dependence on arguments $j < i$) as well as the present inference (the dependence on argument i). Instead, the right notion is a choice of tied parameters such that the model is, aggregated over positions, optimal for the present task when conditioned on a fixed past. That is, forward passes do not compute features for the future if they can compute other features more beneficial to the present.

Definition 3. The parameters $\tilde{\theta}$ are *(tied-)myopic* if they satisfy³

$$\tilde{\theta} \in \arg \min_{\theta} \sum_{i=1}^n \ell_i(\tilde{\theta}, \dots, \tilde{\theta}, \theta). \quad (3)$$

The *(tied) myopia gap* is then defined analogously to Definition 2.

Hypothesis 4 (Breadcrumbs). The myopia gap is small—near-optimal performance can be attained even when each forward pass is computing features relevant to only its own immediate inference task, with no regard to pre-caching for the future.

³Parameters satisfying Equation 3 can be guaranteed to exist under certain conditions; see Theorem 11.

If the breadcrumbs hypothesis does not hold, we say that the model is *pre-caching*. It is important to remember that the ℓ_i depend on a choice of transformer model G and dataset \mathcal{D} . That is, breadcrumbs and pre-caching are properties of the model architecture and the data considered as a whole.

Although a small myopia gap reveals that one can do just as well without pre-caching, it does not say much about any specific model. To measure pre-caching within a given model, we examine the extent to which its parameters violate the myopia constraints.

Definition 5. The *untied local myopia bonus* at $\theta_1^*, \dots, \theta_n^*$ is

$$\sum_{i=1}^n \hat{c}_i(\theta_1^*, \dots, \theta_n^*) := \sum_{i=1}^n \ell_i(\theta_1^*, \dots, \theta_i^*) - \min_{\theta_i} \ell_i(\theta_1^*, \dots, \theta_{i-1}^*, \theta_i) \geq 0.$$

Likewise, the *(tied) local myopia bonus* at θ^* is

$$\hat{c}(\theta^*) := \min_{\theta} \sum_{i=1}^n (\ell_i(\theta^*, \dots, \theta^*) - \ell_i(\theta^*, \dots, \theta^*, \theta)) \geq 0.$$

For further interpretation of the myopia bonus, see Section A.

3.4 Myopic gradient descent

Our heuristic remark in Section 3.2 (that the off-diagonal gradient terms are responsible for pre-caching) is justified by Theorem 13. It states that, given certain conditions on the loss terms ℓ_i , performing gradient descent with the off-diagonal terms removed results in a myopic model in the sense of Definition 3.⁴ We call this *myopic descent*.

For myopic descent to be stable in the tied-weights case, we need, roughly speaking, for the model to depend more on the parameters associated with the present forward pass than those from the past. This is a plausible condition—dependence on the past is mediated by the attention mechanism, which comprises a relatively small fraction of the total parameter count. The precise condition we use is **forward bias**, from Definition 10.

Theorem 13. Let $f(\tilde{\theta}, \theta) := \ell(\tilde{\theta}, \dots, \tilde{\theta}, \theta)$. If f is forward-biased, σ -strongly convex, and L -smooth, then, for some step size $\eta > 0$, the iterates of myopic descent with tied weights

$$\theta^{(t+1)} = \theta^{(t)} - \eta \nabla_{\theta} f(\tilde{\theta}, \theta) \Big|_{\tilde{\theta}=\theta=\theta^{(t)}}$$

converge to $\tilde{\theta} \in \Theta$ satisfying the myopia constraints of Equation 3.

4 Synthetic data experiments

To demonstrate a simple instance where significant pre-caching occurs (and thus the myopia gap is large), we construct the following synthetic dataset.

Definition 6. The data distribution $\mathcal{D}_{p,a,b}^N$ is defined as the joint distribution of real-valued random variables $(x_n)_{n=1}^N, (y_n)_{n=1}^N, (z_n)_{n=1}^N$ where, for each n ,

- $x_n \sim \mathcal{N}(0, 1)$ (standard Gaussian)
- $z_n \sim \text{Ber}(p)$ (Bernoulli with probability p)
- $y_n = z_n \sum_{i=1}^a \sin(bx_{n-i}) + (1 - z_n)x_n$

and $\{x_n\}_{n \in \mathbb{N}} \cup \{z_n\}_{n \in \mathbb{N}}$ are mutually independent. In our experiments, we always set the parameters $a = b = 10$ and $N = 64$, so for convenience notate $\mathcal{D}_p := \mathcal{D}_{p,10,10}^{64}$.

⁴In order to simplify the theory, we prove our results for the strongly convex L -smooth case. These are not entirely artificial assumptions; for example, Milne (2019) shows that certain feedforward neural networks have loss functions that are piecewise strongly convex with respect to their parameters in a neighborhood of all global optima.

The intuition is that a transformer regression model G trained on \mathcal{D}_p would benefit from pre-caching $\sin(bx_n)$ during its forward pass at position n , even though this computation is irrelevant to its task of predicting y_n . One simple strategy that makes use of this pre-caching is Algorithm 1.

The motivation for the Bernoulli variables z_i is that, as p decreases, the expected first time when $\sin(bx_n)$ becomes useful advances further into the future. In addition, when p is sufficiently small, the probability $(1-p)^a$ that the value $\sin(bx_n)$ is never useful at all becomes non-negligible. We will show that, even in this case, the transformer model learns to pre-cache.

Investigating myopia. Suppose that we train a myopic model (Section 3.4) on the same task. Since this model lacks off-diagonal gradient terms, we do not expect it to learn to pre-cache $\sin(bx_n)$ at position n . One possible strategy that does not use pre-caching is Algorithm 2. We expect this brute force algorithm to perform significantly worse given the same parameter count—it computes a b -dimensional nonlinear function within a single layer, while each layer of Algorithm 1 computes only scalar nonlinear functions.⁵

Algorithm 1 Pre-caching algorithm

At position n ,
input x_n, z_n
layer 1 compute $F_n := \sin(bx_n)$
layer 2 read F_{n-i} for $i = 1, \dots, a$.
layer 2 compute
 $\hat{y}_n := z_n \sum_{i=1}^a F_{n-i} + (1 - z_n)x_n$.
return \hat{y}_n .

Algorithm 2 Brute force algorithm

At position n ,
input x_n, z_n
layer 1 compute \emptyset
layer 2 read x_{n-i} for $i = 1, \dots, a$.
layer 2 compute
 $\hat{y}_n := z_n \sum_{i=1}^a \sin(bx_{n-i}) + (1 - z_n)x_n$.
return \hat{y}_n .

4.1 Evaluation: linear probing

To determine if the transformer model is computing $\sin(bx_n)$ at position n , we fit linear probes on the hidden states. We additionally compute the correlations between $\sin(bx_n)$ and each individual dimension (i.e., each neuron) of each hidden state.⁶ See Section E.1 for details.

4.2 Results

For varying p , we train two-layer transformer models with embedding dimensions of 128 on \mathcal{D}_p using using both ordinary and myopic gradient descent. Full architecture and training details are provided in Section E.

From examining the performance of each linear probe against $\sin(bx_{n-i})$ for varying i , we find strong evidence that the transformer model with vanilla training is indeed pre-caching $\sin(bx_n)$, possibly in order to implement Algorithm 1. Indeed, in Figure 2,

- The zeroth hidden state (i.e., the sum of the input and position embeddings) at position n is correlated with only x_n .
- The first hidden state is correlated with $\sin(bx_n)$ but not correlated with any $\sin(bx_{n-i})$ for $i > 0$.

⁵For example, (Shen et al., 2022) provide upper bounds on error that degrade exponentially in dimensionality given a fixed parameter and layer count.

⁶Note that, in order for linear probing to be meaningful, we must first ensure that there is no pre-existing linear relationship between the inputs and the quantities we are probing for. Since the $(x_n, z_n)_n$ are mutually independent, this follows from Lemma 15, stating that x_n and $\sin(bx_n)$ have near-zero correlation for large enough b . In our experiments, we set $b = 10$, in which case $\rho(x_n, \sin(bx_n)) < 10^{-20}$. In other words, there is low predictive \mathcal{V} -information from the inputs to the target $\sin(bx_n)$, where \mathcal{V} is the class of linear models (Xu et al., 2020).

- The second hidden state (immediately before the output unembedding) is correlated with $\sin(bx_{n-i})$ for each $0 \leq i \leq a$.

Further, looking at the per-neuron correlations in Figure 3, we see that $\sin(bx_{n-i})$ for $1 \leq i \leq a$ are all correlated with a single 1-d subspace of the second hidden state (they share the same striping pattern); this is the subspace corresponding to $\sum_{i=1}^a \sin(bx_{n-i})$. Meanwhile, $\sin(bx_n)$, as well as many of the x_{n-i} , are located in various other 1-d subspace of the second hidden state; these terms are all left over in the residual stream from previous layers, and are cleaned up only by the output unembedding.

On the other hand, in Table 1, the myopic models perform significantly worse. The per-neuron correlations in Figure 3 suggest that the myopic model may be implementing a crude approximation of Algorithm 2. This suggests that the synthetic setting has an inherently high *myopia gap*—it is impossible for the transformer model to do well without pre-caching.

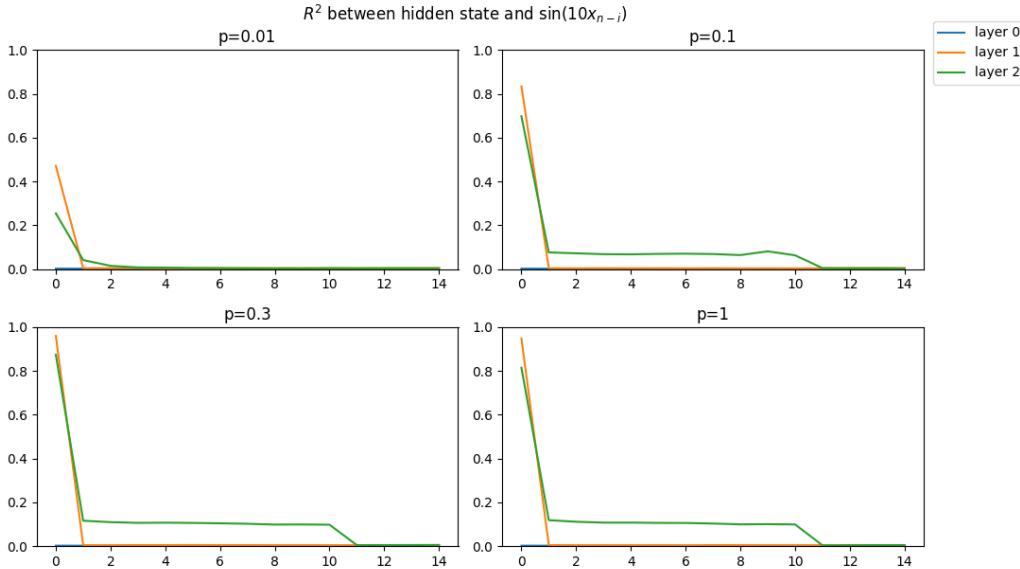


Figure 2: Empirical R^2 between linear probes fit on each layer of vanilla transformer models trained on \mathcal{D}_p for $p \in \{0.01, 0.1, 0.3, 1\}$ to targets $\sin(bx_{n-i})$. Computed over 50 000 samples from \mathcal{D}_1 .

5 Natural language experiments

In order to measure the extent to which transformer models learn to pre-cache on natural language data, we estimate both the myopia gap (Definition 3) of this setting as well as the local myopia bonus (Definition 5) of a transformer model with vanilla training. All models use the 124M-parameter GPT-2 architecture; see Table 4 for configuration details.

We train all models (vanilla and myopic) from random initialization for one epoch on 4.6M sequences from the MS MARCO dataset (Nguyen et al., 2016), truncated to length 64. To estimate the local myopia bonus of the vanilla model, we train another model from random initialization with the same architecture, but with past hidden states provided by the vanilla model; see Section C for details.⁷

As baseline, we also train a “transformer bigram” model, a model with an identical architecture but all off-diagonal key/value states zeroed out.

⁷Here, we do not use any existing pre-trained models (outside of the pre-trained tokenizer) for our experiments. This choice was made to avoid the interference of distribution shift and varying training schemes when comparing between the vanilla and myopic models.

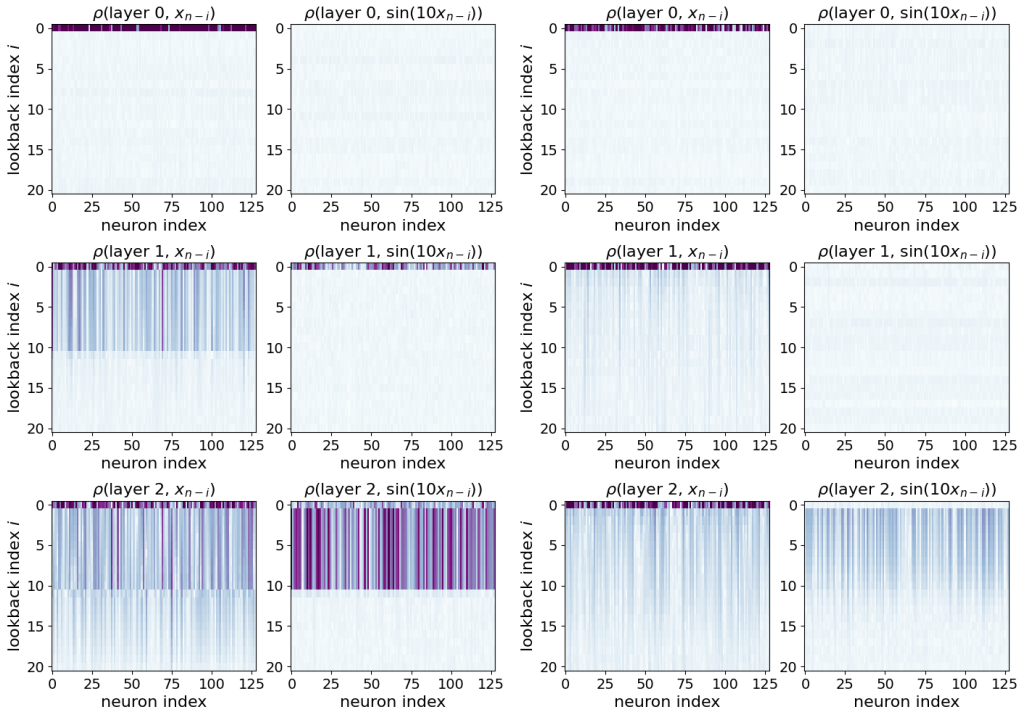


Figure 3: Per-neuron empirical correlation between linear probes fit on each layer of vanilla (left two columns) and myopic (right two) models each trained on $\mathcal{D}_{0.3}$ to targets x_{n-i} and $\sin(bx_{n-i})$. Values are truncated to $[0, 0.25]$.

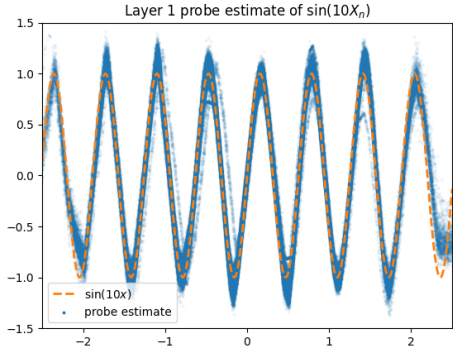


Figure 4: Estimate of $\sin(bx_n)$ by linear probe fit on layer 1 of transformer with vanilla training on $\mathcal{D}_{0.3}$. Computed over 50 000 samples from \mathcal{D}_1 .

5.1 Results

From Table 2, the estimated myopia gap in this setting is $3.40 - 3.28 = 0.12$, while the local myopia bonus of the vanilla model is $3.28 - 3.26 = 0.02$.

The somewhat nonnegligible myopia gap suggests that pre-caching may provide a small nonzero benefit. Indeed, in Figure 5, we see that the myopic model outperforms the vanilla model at the beginning of the sequence, but falls behind as the length of the past increases. This implies that a lack of pre-caching may compound, and model performance degrades later in the sequence as the model is unable to refer to prior pre-cached information.

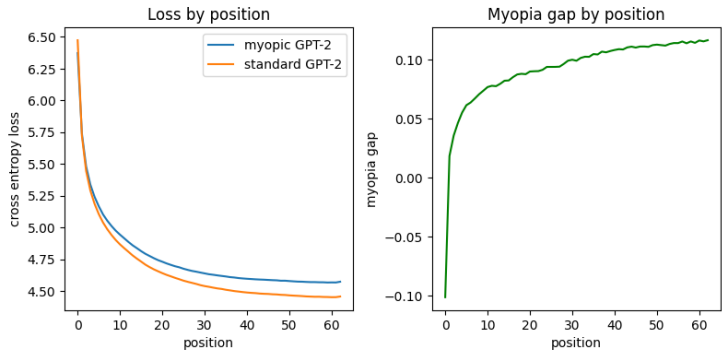


Figure 5: Cross-entropy loss of vanilla and myopic GPT-2 models by token position, and their difference. Evaluated on a sliding window over a 100K-token sample text from the PG-19 dataset (Rae et al., 2019). Aggregate cross-entropy losses on this sample are 4.67 (vanilla) and 4.77 (myopic).

However, note that this gap is much smaller than that between the vanilla model and the transformer bigram model. That is, the myopic model is still able to leverage past information (breadcrumbs) to a significant extent, even if they optimized only for the present inference task.

That the local myopia gap is near zero further supports this direction—the model learned through vanilla training does not trade off significantly between features useful for the present and pre-caching for the future.

p	Vanilla	Myopic
0.01	0.096	1.10
0.1	0.016	0.97
0.3	0.0030	1.03
1.0	0.0074	1.26

Table 1: Normalized Huber loss \mathcal{L}/p for vanilla and myopic models trained and evaluated on \mathcal{D}_p for each p in our synthetic setting. For reference, the trivial model that always outputs zero attains a Huber loss of 1.26.

Model	Cross-entropy
Vanilla	3.28
Myopic	3.40
Local myopic	3.26
Transformer bigram	5.33

Table 2: Validation cross-entropy loss obtained by GPT-2 with vanilla and myopic training

6 Conclusion

We consider the phenomenon where transformer language models compute features in the present that are then relevant to the future. We propose two possible explanations, breadcrumbs and pre-caching. Using a synthetic dataset, we demonstrate that pre-caching does indeed occur in the transformer model. On the other hand, our experiments with natural language models suggest that breadcrumbs is more explanatory in that setting.

Acknowledgments

LL thanks Lukas Berglund and David Schneider-Joseph for inspiring conversations. This research was partly supported by Open Philanthropy and the Berkeley Existential Risk Initiative.

References

- Maik Barthel, Sebastian Sauppe, Stephen C Levinson, and Antje S Meyer. The timing of utterance planning in task-oriented dialogue: Evidence from a novel list-completion paradigm. *Frontiers in psychology*, 7:1858, December 2016. doi: 10.3389/fpsyg.2016.01858.
- David Bau, Jun-Yan Zhu, Hendrik Strobelt, Agata Lapedriza, Bolei Zhou, and Antonio Torralba. Understanding the role of individual units in a deep neural network. *Proceedings of the National Academy of Sciences*, 117(48):30071–30078, September 2020. ISSN 1091-6490. doi: 10.1073/pnas.1907375117. URL <http://dx.doi.org/10.1073/pnas.1907375117>.
- Amir Beck. *First-Order Methods in Optimization*. Society for Industrial and Applied Mathematics, Philadelphia, PA, 2017. doi: 10.1137/1.9781611974997. URL <https://epubs.siam.org/doi/abs/10.1137/1.9781611974997>.
- Yonatan Belinkov. Probing classifiers: Promises, shortcomings, and advances, 2021.
- Yonatan Belinkov and James Glass. Analysis methods in neural language processing: A survey, 2019.
- Nora Belrose, Zach Furman, Logan Smith, Danny Halawi, Igor Ostrovsky, Lev McKinney, Stella Biderman, and Jacob Steinhardt. Eliciting latent predictions from transformers with the tuned lens, 2023.
- Tianle Cai, Yuhong Li, Zhengyang Geng, Hongwu Peng, Jason D. Lee, Deming Chen, and Tri Dao. Medusa: Simple llm inference acceleration framework with multiple decoding heads, 2024.
- Alexander Yom Din, Taelin Karidi, Leshem Choshen, and Mor Geva. Jump to conclusions: Short-cutting transformers with linear transformations, 2023.
- Evan Hernandez, Arnab Sen Sharma, Tal Haklay, Kevin Meng, Martin Wattenberg, Jacob Andreas, Yonatan Belinkov, and David Bau. Linearity of relation decoding in transformer language models, 2024.
- John Hewitt and Percy Liang. Designing and interpreting probes with control tasks, 2019.
- Thak Yin Hu and W. A. Kirk. Local contractions in metric spaces. *Proceedings of the American Mathematical Society*, 68(1):121–124, 1978. ISSN 00029939, 10886826. URL <http://www.jstor.org/stable/2040922>.
- Falk Huettig. Four central questions about prediction in language processing. *Brain Research*, 1626:118–135, 2015. ISSN 0006-8993. doi: <https://doi.org/10.1016/j.brainres.2015.02.014>. URL <https://www.sciencedirect.com/science/article/pii/S0006899315001146>. Predictive and Attentive Processing in Perception and Action.
- Kenneth Li, Aspen K. Hopkins, David Bau, Fernanda Viégas, Hanspeter Pfister, and Martin Wattenberg. Emergent world representations: Exploring a sequence model trained on a synthetic task, 2023.
- Kevin Meng, David Bau, Alex Andonian, and Yonatan Belinkov. Locating and editing factual associations in gpt, 2023.
- George A. Miller. *Language and communication*. McGraw-Hill, New York, NY, US, 1951. doi: 10.1037/11135-000.

- Tristan Milne. Piecewise strong convexity of neural networks. In H. Wallach, H. Larochelle, A. Beygelzimer, F. d'Alché-Buc, E. Fox, and R. Garnett (eds.), *Advances in Neural Information Processing Systems*, volume 32. Curran Associates, Inc., 2019. URL https://proceedings.neurips.cc/paper_files/paper/2019/file/b33128cb0089003ddfb5199e1b679652-Paper.pdf.
- Neel Nanda, Lawrence Chan, Tom Lieberum, Jess Smith, and Jacob Steinhardt. Progress measures for grokking via mechanistic interpretability, 2023.
- Yurii Nesterov. *Lectures on Convex Optimization*. Springer Publishing Company, Incorporated, 2nd edition, 2018. ISBN 3319915770.
- Tri Nguyen, Mir Rosenberg, Xia Song, Jianfeng Gao, Saurabh Tiwary, Rangan Majumder, and Li Deng. MS MARCO: A human generated machine reading comprehension dataset. In Tarek Richard Besold, Antoine Bordes, Artur S. d'Avila Garcez, and Greg Wayne (eds.), *Proceedings of the Workshop on Cognitive Computation: Integrating neural and symbolic approaches 2016 co-located with the 30th Annual Conference on Neural Information Processing Systems (NIPS 2016), Barcelona, Spain, December 9, 2016*, volume 1773 of *CEUR Workshop Proceedings*. CEUR-WS.org, 2016. URL https://ceur-ws.org/Vol-1773/CoCoNIPS_2016_paper9.pdf.
- nostalgebraist. Interpreting gpt: The logit lens, 2020.
- Chris Olah, Nick Cammarata, Ludwig Schubert, Gabriel Goh, Michael Petrov, and Shan Carter. Zoom in: An introduction to circuits. *Distill*, 2020. doi: 10.23915/distill.00024.001. <https://distill.pub/2020/circuits/zoom-in>.
- Koyena Pal, Jiuding Sun, Andrew Yuan, Byron Wallace, and David Bau. Future lens: Anticipating subsequent tokens from a single hidden state. In *Proceedings of the 27th Conference on Computational Natural Language Learning (CoNLL)*. Association for Computational Linguistics, 2023. doi: 10.18653/v1/2023.conll-1.37. URL <http://dx.doi.org/10.18653/v1/2023.conll-1.37>.
- Tiago Pimentel, Josef Valvoda, Rowan Hall Maudslay, Ran Zmigrod, Adina Williams, and Ryan Cotterell. Information-theoretic probing for linguistic structure, 2020.
- Jack W Rae, Anna Potapenko, Siddhant M Jayakumar, Chloe Hillier, and Timothy P Lillicrap. Compressive transformers for long-range sequence modelling. *arXiv preprint*, 2019. URL <https://arxiv.org/abs/1911.05507>.
- Zuowei Shen, Haizhao Yang, and Shijun Zhang. Optimal approximation rate of relu networks in terms of width and depth. *Journal de Mathématiques Pures et Appliquées*, 157: 101–135, 2022. ISSN 0021-7824. doi: <https://doi.org/10.1016/j.matpur.2021.07.009>. URL <https://www.sciencedirect.com/science/article/pii/S0021782421001124>.
- Xing Shi, Inkit Padhi, and Kevin Knight. Does string-based neural mt learn source syntax? pp. 1526–1534, 01 2016. doi: 10.18653/v1/D16-1159.
- Ashish Vaswani, Noam Shazeer, Niki Parmar, Jakob Uszkoreit, Llion Jones, Aidan N Gomez, Łukasz Kaiser, and Illia Polosukhin. Attention is all you need. In *Advances in Neural Information Processing Systems*, volume 30. Curran Associates, Inc., 2017. URL https://proceedings.neurips.cc/paper_files/paper/2017/file/3f5ee243547dee91fbd053c1c4a845aa-Paper.pdf.
- Yilun Xu, Shengjia Zhao, Jiaming Song, Russell Stewart, and Stefano Ermon. A theory of usable information under computational constraints, 2020.
- Ziqian Zhong, Ziming Liu, Max Tegmark, and Jacob Andreas. The clock and the pizza: Two stories in mechanistic explanation of neural networks, 2023.

A Myopia bonus and malus

Notice that the myopia gap consists of two pieces: a *myopia bonus*, the improvement that can be obtained at the current forward pass by ignoring the future forward passes; and a *myopia malus*, the cost to the future forward passes that is incurred by not pre-caching for them. To be precise, in the untied case,⁸ given a choice of myopic $\tilde{\theta}_1, \dots, \tilde{\theta}_n$ satisfying constraints (1) of Definition 1, write

$$\begin{aligned} & \ell(\tilde{\theta}_1, \dots, \tilde{\theta}_n) - \min_{\theta_1, \dots, \theta_n} \ell(\theta_1, \dots, \theta_n) \\ &= \sum_{i=1}^n \left(\min_{\theta_1, \dots, \theta_n} \ell(\tilde{\theta}_1, \dots, \tilde{\theta}_{i-1}, \tilde{\theta}_i, \theta_{i+1}, \dots, \theta_n) - \min_{\theta_{i+1}, \dots, \theta_n} \ell(\tilde{\theta}_1, \dots, \tilde{\theta}_{i-1}, \theta_i, \theta_{i+1}, \dots, \theta_n) \right) \\ &= \sum_{i=1}^n (\ell_i(\tilde{\theta}_1, \dots, \tilde{\theta}_{n-1}, \tilde{\theta}_i) - \ell_i(\tilde{\theta}_1, \dots, \tilde{\theta}_{n-1}, \theta_i^{*i})) \\ & \quad + \sum_{i=1}^n \sum_{j=i+1}^n \left(\ell_j(\tilde{\theta}_1, \dots, \tilde{\theta}_{i-1}, \tilde{\theta}_i, \theta_{i+1}^{*i+1}, \dots, \theta_n^{*i+1}) - \ell_j(\tilde{\theta}_1, \dots, \tilde{\theta}_{i-1}, \theta_i^{*i}, \theta_{i+1}^{*i}, \dots, \theta_n^{*i}) \right). \end{aligned}$$

where we define

$$\theta_i^{*i}, \dots, \theta_n^{*i} \in \arg \min_{\theta_1, \dots, \theta_n} \ell(\tilde{\theta}_1, \dots, \tilde{\theta}_{i-1}, \theta_i, \theta_{i+1}, \dots, \theta_n).$$

That is, the myopia gap is the sum $c + d = \sum_i c_i + \sum_i d_i$ of the differences between the myopia bonuses

$$c_i(\tilde{\theta}_1, \dots, \tilde{\theta}_n) := \ell_i(\tilde{\theta}_1, \dots, \tilde{\theta}_{n-1}, \theta_i^{*i}) - \ell_i(\tilde{\theta}_1, \dots, \tilde{\theta}_{n-1}, \tilde{\theta}_i) \geq 0$$

and the myopia maluses

$$\begin{aligned} & d_i(\tilde{\theta}_1, \dots, \tilde{\theta}_n) \\ &:= \sum_{j=i+1}^n \left(\ell_j(\tilde{\theta}_1, \dots, \tilde{\theta}_{i-1}, \tilde{\theta}_i, \theta_{i+1}^{*i+1}, \dots, \theta_n^{*i+1}) - \ell_j(\tilde{\theta}_1, \dots, \tilde{\theta}_{i-1}, \theta_i^{*i}, \theta_{i+1}^{*i}, \dots, \theta_n^{*i}) \right) \\ &\geq 0, \end{aligned}$$

with $d_i - c_i \geq 0$ for each $1 \leq i \leq n$. *A priori*, a small myopia gap does not necessarily imply a small myopia bonus c and malus d . Indeed, in the case when the myopia gap is small, a large value for c (and thus a corresponding large value for d) means precisely that the transformer model is committing significant resources to pre-caching that could otherwise have been used to improve inference on the current position. On the other hand, it is possible that both c and d are small; that is, there is not much cost associated with pre-caching for the future, as the present forward pass already results in information (breadcrumbs) useful for that purpose.

In practice, the myopia bonus may be difficult to estimate, as it depends on the result of $O(n)$ separate optimization problems (each of which, in practice, is a full transformer model training run). Thus, we instead compute the local myopia bonus of Definition 5.

B Making the breadcrumbs explicit

In practice, the dependence of forward pass G_i on previous forward passes G_j for $j < i$ is mediated through hidden states h_1, \dots, h_{i-1} :

$$G_i(\mathbf{x}_1, \dots, \mathbf{x}_i; \theta_1, \dots, \theta_i) = \hat{G}_i(h_1, \dots, h_{i-1}, \mathbf{x}_i; \theta_i)$$

where the h_i are themselves recursively defined parameterized functions $h_i = h_i(h_1, \dots, h_{i-1}, \mathbf{x}_i; \theta_i)$. (Note that we are making a choice here to consider transformers

⁸The tied case is exactly analogous, so we do not write it explicitly.

as functions of hidden states, and not their key/value states. This has implications for how myopic descent is defined: when hidden state \mathbf{h}_j is attended to by forward pass $i > j$, we consider the key and value weights \mathbf{W}_K and \mathbf{W}_V , respectively, to belong to forward pass i . Thus, they are updated by the gradient wrt. ℓ_i .)

With the hidden states explicitly written out, the gradient wrt. the loss is a sum over all possible paths to the present: for $j < i$,

$$\frac{\partial G_i}{\partial \theta_j}(\mathbf{x}_1, \dots, \mathbf{x}_i; \theta_1, \dots, \theta_i) = \sum_{j=i_1 < \dots < i_m < i} \frac{\partial \mathbf{h}_j}{\partial \theta_j} \frac{\partial \hat{G}_i}{\mathbf{h}_{i_m}} \prod_{k=1}^{m-1} \frac{\partial \mathbf{h}_{i_k}}{\partial \mathbf{h}_{i_{k-1}}}.$$

where the sum is over all partitions $j = i_1 < \dots < i_m < i$.

C The myopic attention mechanism

A primitive that we use when implementing both the myopic gradient descent of Section 3.4 and the local myopic bonus of Definition 5 is an attention mechanism that uses key/value states for past forward passes differing from those it uses for the current pass, while still computing all forward passes in parallel. For myopic descent, the alternate key/value states are the result of key/value weights \mathbf{W}_K and \mathbf{W}_V , respectively, multiplying a cloned and detached copy of the previous hidden states. When computing the local myopic bonus, the alternate key/value states come from a separate pre-trained transformer model.

Let $\mathbf{X} = (\mathbf{x}_1, \dots, \mathbf{x}_n)^\top \in \mathbb{R}^{n \times d}$ be the input sequence of embedded tokens, with each row representing one token embedded in \mathbb{R}^d . Let $\mathbf{W}_Q, \mathbf{W}_K, \mathbf{W}_V \in \mathbb{R}^{d \times d}$ be the query, key, value weight matrices for one attention head of the transformer G . Denote

$$\tilde{\mathbf{Q}} := \mathbf{X}\mathbf{W}_Q, \tilde{\mathbf{K}} := \tilde{\mathbf{X}}\mathbf{W}_K, \mathbf{V} := \mathbf{X}\mathbf{W}_V$$

and let $\mathbf{Q}, \mathbf{K}, \mathbf{V}$ be the alternate states we wish to use for off-diagonal attention terms. We adopt the convention that lowercase letters with subscripts represent rows of matrices; e.g. q_i is the i th row of \mathbf{Q} .

Recall that the vanilla attention pass for G is

$$\mathbf{Y} = \sigma(\mathbf{Q}\mathbf{K}^\top)\mathbf{V},$$

where σ is row-wise softmax. Writing this out token-wise,

$$\mathbf{y}_i = Z_i^{-1} \sum_{j=1}^n \exp(q_i^\top \mathbf{k}_j) \mathbf{v}_j,$$

where Z_i is the partition function

$$Z_i := \sum_{j=1}^n \exp(q_i^\top \mathbf{k}_j).$$

The myopic attention mechanism, on the other hand, written tokenwise, is

$$\begin{aligned} \tilde{\mathbf{y}}_i &= \tilde{Z}_i^{-1} \left(\exp(\tilde{q}_i^\top \tilde{\mathbf{k}}_i) \tilde{\mathbf{v}}_i + \sum_{j \neq i} \exp(\tilde{q}_i^\top \mathbf{k}_j) \mathbf{v}_j \right) \\ &= \tilde{Z}_i^{-1} \sum_{j=1}^n \exp(\tilde{q}_i^\top \mathbf{k}_j + \delta_{ij} \tilde{q}_i^\top (\tilde{\mathbf{k}}_j - \mathbf{k}_j)) (\mathbf{v}_j + \delta_{ij} (\tilde{\mathbf{v}}_j - \mathbf{v}_j)) \\ &= \sum_{j=1}^n a_{ij} \mathbf{v}_j - \sum_{j=1}^n \delta_{ij} a_{ij} (\tilde{\mathbf{v}}_j - \mathbf{v}_j) \end{aligned}$$

where

$$\begin{aligned}\tilde{Z}_i &:= \exp(\tilde{\mathbf{q}}_i^\top \tilde{\mathbf{k}}_i) + \sum_{j \neq i} \exp(\tilde{\mathbf{q}}_i^\top \mathbf{k}_j) \\ &= \sum_{j=1}^n \exp(\tilde{\mathbf{q}}_i^\top \mathbf{k}_j + \delta_{ij} \tilde{\mathbf{q}}_i^\top (\tilde{\mathbf{k}}_j - \mathbf{k}_j)), \\ a_{ij} &:= \tilde{Z}_i^{-1} \exp(\tilde{\mathbf{q}}_i^\top \mathbf{k}_j + \delta_{ij} \tilde{\mathbf{q}}_i^\top (\tilde{\mathbf{k}}_j - \mathbf{k}_j)),\end{aligned}$$

and δ_{ij} is the Kronecker delta. Now, denote

$$(\text{diag } \mathbf{A})_{ij} := \delta_{ij} A_{ij}.$$

That is, $\text{diag } \mathbf{A}$ is the diagonal matrix that has the same entries as \mathbf{A} along the diagonal and is zero elsewhere. We are now able to write the above in matrix form:

$$\tilde{\mathbf{Y}} = \mathbf{A}\mathbf{V} + (\text{diag } \mathbf{A})(\tilde{\mathbf{V}} - \mathbf{V}),$$

where

$$\mathbf{A} := \sigma(\tilde{\mathbf{Q}}\mathbf{K}^\top + \text{diag}(\tilde{\mathbf{Q}}(\tilde{\mathbf{K}}^\top - \mathbf{K}^\top))).$$

D Proofs

D.1 Gradient descent with untied weights

Theorem 7. Assume $\ell: \Theta^n \rightarrow \mathbb{R}$ is σ -strongly convex and L -smooth. Consider ordinary gradient descent with untied weights

$$\boldsymbol{\theta}_i^{(t)} = \boldsymbol{\theta}_i^{(t-1)} - \eta \nabla_{\boldsymbol{\theta}_i} \ell(\boldsymbol{\theta}_1^{(t-1)}, \dots, \boldsymbol{\theta}_i^{(t-1)}) \quad \forall i \in \{1, \dots, n\}.$$

Then, for $\boldsymbol{\theta}_1^*, \dots, \boldsymbol{\theta}_n^* = \arg \min_{\boldsymbol{\theta}_1, \dots, \boldsymbol{\theta}_n} \ell(\boldsymbol{\theta}_1, \dots, \boldsymbol{\theta}_n)$, for small enough $\eta > 0$,

$$\|\boldsymbol{\theta}_i^{(t)} - \boldsymbol{\theta}_i^*\|_2^2 \leq \left(1 - \frac{2\eta\sigma L}{\sigma + L}\right)^t \|\boldsymbol{\theta}_i^{(0)} - \boldsymbol{\theta}_i^*\|_2^2 \quad \forall i \in \{1, \dots, n\}.$$

Proof. This is a standard convergence result for gradient descent on strongly convex functions. For example, see (Nesterov, 2018). \square

D.2 Gradient descent with tied weights

Theorem 8. Assume ℓ is σ -strongly convex and L -smooth, and consider ordinary gradient descent with tied weights

$$\begin{aligned}\boldsymbol{\theta}_1^{(0)} &= \dots = \boldsymbol{\theta}_n^{(0)} \\ \boldsymbol{\theta}_i^{(t+1)} &= \boldsymbol{\theta}_i^{(t)} + \eta \sum_{i=1}^n \nabla_{\boldsymbol{\theta}_i} \ell(\boldsymbol{\theta}_1, \dots, \boldsymbol{\theta}_n) \quad \forall i \in \{1, \dots, n\}.\end{aligned}$$

There exists $\eta > 0$ such that

$$\|\boldsymbol{\theta}_i^{(t)} - \boldsymbol{\theta}^*\|_2^2 \leq \left(1 - \frac{2\eta n \sigma L}{\sigma + L}\right)^t \|\boldsymbol{\theta}_i^{(0)} - \boldsymbol{\theta}^*\|_2^2 \quad \forall i \in \{1, \dots, n\}.$$

where $\boldsymbol{\theta}^* = \arg \min_{\boldsymbol{\theta}} \ell(\boldsymbol{\theta}, \dots, \boldsymbol{\theta})$.

Proof. This is again the standard convergence result, now applied to the σ -strongly convex $\sqrt{n}L$ -smooth function $\boldsymbol{\theta} \mapsto \ell(\boldsymbol{\theta}/\sqrt{n}, \dots, \boldsymbol{\theta}/\sqrt{n})$. Alternatively, one may think of this as projected gradient descent constrained to the subspace $\boldsymbol{\theta}_1 = \dots = \boldsymbol{\theta}_n$ with a step size of $n\eta$. Projected gradient descent inherits the same convergence properties as unconstrained gradient descent (Beck, 2017). \square

D.3 Myopic descent with untied weights

Theorem 9. Assume each of the ℓ_1, \dots, ℓ_n are σ -strongly convex and L -smooth. Consider myopic gradient descent with untied weights

$$\boldsymbol{\theta}_i^{(t)} = \boldsymbol{\theta}_i^{(t-1)} - \eta \nabla_{\boldsymbol{\theta}_i} \ell_i(\boldsymbol{\theta}_1^{(t-1)}, \dots, \boldsymbol{\theta}_i^{(t-1)}) \quad \forall i \in \{1, \dots, n\}.$$

There exists $\eta > 0$ such that $\boldsymbol{\theta}_i \xrightarrow{t \rightarrow \infty} \tilde{\boldsymbol{\theta}}_i$ for all i , where

$$\begin{aligned} \tilde{\boldsymbol{\theta}}_1 &= \arg \min_{\boldsymbol{\theta}_1} \ell_1(\boldsymbol{\theta}_1) \\ \tilde{\boldsymbol{\theta}}_2 &= \arg \min_{\boldsymbol{\theta}_2} \ell_2(\tilde{\boldsymbol{\theta}}_1, \boldsymbol{\theta}_2) \\ &\dots \\ \tilde{\boldsymbol{\theta}}_n &= \arg \min_{\boldsymbol{\theta}_n} \ell_n(\tilde{\boldsymbol{\theta}}_1, \tilde{\boldsymbol{\theta}}_2, \dots, \tilde{\boldsymbol{\theta}}_{n-1}, \boldsymbol{\theta}_n). \end{aligned}$$

Proof. Let $\tilde{\boldsymbol{\theta}}_1, \dots, \tilde{\boldsymbol{\theta}}_n$ be as in the theorem statement. We proceed by induction. For the base case, note that the myopic descent iterates for $\boldsymbol{\theta}_1^{(t)}$ are independent of $\boldsymbol{\theta}_j^{(t)}$ for $j > 1$. Thus, the standard convergence theorem gives that $\boldsymbol{\theta}_1^{(t)} \rightarrow \tilde{\boldsymbol{\theta}}_1$ as $t \rightarrow \infty$.

Now, assume $\boldsymbol{\theta}_i^{(t)} \xrightarrow{t \rightarrow \infty} \tilde{\boldsymbol{\theta}}_i$ for all $i < k$. Thus, for any $\varepsilon > 0$, for sufficiently large t ,

$$\|(\boldsymbol{\theta}_i^{(t)})_{i=1}^{k-1} - (\tilde{\boldsymbol{\theta}}_i)_{i=1}^{k-1}\|_2 < \varepsilon.$$

Thus, since ℓ_k is L -smooth, for any $\boldsymbol{\theta}_k$,

$$\|\nabla_{\boldsymbol{\theta}_k} \ell_k(\boldsymbol{\theta}_1^{(t)}, \dots, \boldsymbol{\theta}_{k-1}^{(t)}, \boldsymbol{\theta}_k) - \nabla_{\boldsymbol{\theta}_k} \ell_k(\tilde{\boldsymbol{\theta}}_1, \dots, \tilde{\boldsymbol{\theta}}_{k-1}, \boldsymbol{\theta}_k)\|_2 < L\varepsilon.$$

That is,

$$\langle \nabla_{\boldsymbol{\theta}_k} \ell_k(\boldsymbol{\theta}_1^{(t)}, \dots, \boldsymbol{\theta}_{k-1}^{(t)}, \boldsymbol{\theta}_k), \nabla_{\boldsymbol{\theta}_k} \ell_k(\tilde{\boldsymbol{\theta}}_1, \dots, \tilde{\boldsymbol{\theta}}_{k-1}, \boldsymbol{\theta}_k) \rangle \geq \frac{1}{2} \|\nabla_{\boldsymbol{\theta}_k} \ell_k(\tilde{\boldsymbol{\theta}}_1, \dots, \tilde{\boldsymbol{\theta}}_{k-1}, \boldsymbol{\theta}_k)\|_2^2 - \frac{1}{2} L^2 \varepsilon^2$$

is bounded away from zero as long as, say,

$$\|\nabla_{\boldsymbol{\theta}_k} \ell_k(\tilde{\boldsymbol{\theta}}_1, \dots, \tilde{\boldsymbol{\theta}}_{k-1}, \boldsymbol{\theta}_k)\|_2 \geq \sigma \|\boldsymbol{\theta}_k - \tilde{\boldsymbol{\theta}}_k\|_2 > (L+1)\varepsilon,$$

using the σ -strong convexity of ℓ_k . That is, as long as $\|\boldsymbol{\theta}_k - \tilde{\boldsymbol{\theta}}_k\|_2 > \frac{(L+1)\varepsilon}{\sigma}$, it is guaranteed that $-\nabla_{\boldsymbol{\theta}_k} \ell_k(\boldsymbol{\theta}_1^{(t)}, \dots, \boldsymbol{\theta}_{k-1}^{(t)}, \boldsymbol{\theta}_k)$ is a descent direction for $\ell_k(\tilde{\boldsymbol{\theta}}_1, \dots, \tilde{\boldsymbol{\theta}}_{k-1}, \boldsymbol{\theta}_k)$. This is a sufficient condition for $\boldsymbol{\theta}_k$ to converge to a $\frac{(L+1)\varepsilon}{\sigma}$ -neighborhood of $\tilde{\boldsymbol{\theta}}_k$ given a small enough step size (Beck, 2017). Since $\varepsilon > 0$ is arbitrary, this completes the inductive step. \square

D.4 Existence of myopic solutions

Definition 10. A function $f(\mathbf{x}, \mathbf{y}) : \mathbb{R}^a \times \mathbb{R}^b \rightarrow \mathbb{R}$ with continuous second derivatives is **forward-biased** if there exists $\rho < 1$ such that, for all $(\mathbf{x}, \mathbf{y}) \in \mathbb{R}^a \times \mathbb{R}^b$,

$$\|\mathbf{H}_{\mathbf{y}, \mathbf{y}}^{-1}(\mathbf{x}, \mathbf{y}) \mathbf{H}_{\mathbf{y}, \mathbf{x}}(\mathbf{x}, \mathbf{y})\| \leq \rho$$

(in particular, $\mathbf{H}_{\mathbf{y}, \mathbf{y}} \succ 0$ everywhere) where we write the Hessian of f as a block matrix.

$$\mathbf{H}f(\mathbf{x}, \mathbf{y}) = \begin{bmatrix} \mathbf{H}_{\mathbf{x}, \mathbf{x}} f(\mathbf{x}, \mathbf{y}) & \mathbf{H}_{\mathbf{x}, \mathbf{y}} f(\mathbf{x}, \mathbf{y}) \\ \mathbf{H}_{\mathbf{y}, \mathbf{x}} f(\mathbf{x}, \mathbf{y}) & \mathbf{H}_{\mathbf{y}, \mathbf{y}} f(\mathbf{x}, \mathbf{y}) \end{bmatrix} = \begin{bmatrix} \left(\frac{\partial f(\mathbf{x}, \mathbf{y})}{\partial x_i \partial x_j} \right)_{\substack{1 \leq i \leq a \\ 1 \leq j \leq a}} & \left(\frac{\partial f(\mathbf{x}, \mathbf{y})}{\partial x_i \partial y_j} \right)_{\substack{1 \leq i \leq a \\ 1 \leq j \leq b}} \\ \left(\frac{\partial f(\mathbf{x}, \mathbf{y})}{\partial y_i \partial x_j} \right)_{\substack{1 \leq i \leq b \\ 1 \leq j \leq a}} & \left(\frac{\partial f(\mathbf{x}, \mathbf{y})}{\partial y_i \partial y_j} \right)_{\substack{1 \leq i \leq b \\ 1 \leq j \leq b}} \end{bmatrix}$$

Theorem 11. If $f(x, y): \mathbb{R}^a \times \mathbb{R}^a \rightarrow \mathbb{R}$ is forward-biased and strongly convex, then there exists $\tilde{y} \in \mathbb{R}^b$ such that

$$\tilde{y} = \arg \min_{y \in \mathbb{R}^a} f(\tilde{y}, y).$$

Lemma 12. Let $x \in \mathbb{R}^a, y \in \mathbb{R}^b, B \in \mathbb{R}^{a \times b}, C \in \mathbb{R}^{b \times b}$. Then, if $\|x\|_2 \leq c\|y\|_2$ for $c > 0$ and C is symmetric positive-definite, then

$$-c\|BC^{-1}\|y^\top Cy \leq x^\top By \leq c\|BC^{-1}\|y^\top Cy,$$

where for matrices $\|\cdot\|$ is the ℓ_2 operator norm.

Proof. If $y = 0$, then the statement is obvious. Otherwise,

$$\max_{\|x\|_2 \leq c\|y\|_2} \frac{x^\top By}{y^\top Cy} = \max_y \frac{c\|y\|_2 \|By\|_2}{y^\top Cy} \quad (4)$$

$$= \max_y \frac{c\|C^{-1}y\|_2 \|BC^{-1}y\|_2}{y^\top C^{-1}y} \quad (5)$$

$$\leq \max_y \frac{c\|C^{-1}y\|_2}{\|y\|_2} \frac{y^\top y}{y^\top C^{-1}y} \|BC^{-1}\| \quad (6)$$

$$\leq c\|BC^{-1}\|. \quad (7)$$

where (4) is Cauchy-Schwarz, (5) is by reparameterizing y with $C^{-1}y$, (6) is by the definition of the operator norm, and (7) is by diagonalizing C and using that the ℓ_2 norm is bounded above by the ℓ_1 norm. \square

Proof of Theorem 11. Consider the function $g(x) = \arg \min_y f(x, y)$. It is well-defined: each $\arg \min_y f(x, y)$ exists and is unique, since each slice $f(x, -)$ of the strongly convex function f is itself strongly convex. Our goal is to show that g is a local radial contraction, i.e. that there exists $\kappa < 1$ such that each $x \in \mathbb{R}^a$ is contained in an open neighborhood U_x with

$$\|g(x) - g(x')\|_2 \leq \kappa \|x - x'\|_2$$

for all $x' \in U_x$. It then follows (Hu & Kirk, 1978) that g has a unique fixed point \tilde{y}

$$\tilde{y} = g(\tilde{y}) = \arg \min_{y \in \mathbb{R}^a} f(\tilde{y}, y)$$

as desired.

Towards this end, let $x_0 \in \mathbb{R}^a$ be arbitrary and let $y_0 = g(x_0)$. Using the mean value theorem and the continuous second-differentiability of f , for any $x \in \mathbb{R}^a$, there exists $\alpha \in [0, 1]$ such that

$$\begin{aligned} \nabla_y f(x_0 + x, y_0) &= \nabla_y f(x_0, y_0) + H_{y,x} f(x_0 + \alpha x, y_0) x \\ &= H_{y,x} f(x_0 + \alpha x, y_0) x, \end{aligned}$$

where $\nabla_y f(x_0, y_0) = 0$ since $y_0 = g(x_0)$. Now, for any $y \in \mathbb{R}^a$, Taylor's theorem yields

$$\begin{aligned} f(x_0 + x, y_0 + y) &= f(x_0 + x, y_0) + \nabla_y f(x_0 + x, y_0)^\top y + \frac{1}{2} y^\top H_{y,y} f(x_0 + x, y_0 + \beta y) y \\ &= f(x_0 + x, y_0) + x^\top H_{x,y} f(x_0 + \alpha x, y_0) y + \frac{1}{2} y^\top H_{y,y} f(x_0 + x, y_0 + \beta y) y \end{aligned} \quad (8)$$

for some $\beta \in [0, 1]$. On the other hand, by assumption f is σ -strongly convex for some $\sigma > 0$, which gives a lower bound

$$\begin{aligned} f(x_0 + x, y_0 + y) &\geq f(x_0 + x, y_0) + \nabla_y f(x_0 + x, y_0)^\top y + \frac{\sigma}{2} y^\top y \\ &= f(x_0 + x, y_0) + x^\top H_{x,y} f(x_0 + \alpha x, y_0) y + \frac{\sigma}{2} y^\top y. \end{aligned}$$

Applying Lemma 12 to the case $\mathbf{B} = \mathbf{H}_{x,y}f(x_0 + \alpha x, \mathbf{y}_0)$ and $\mathbf{C} = \frac{\sigma}{2}\mathbf{I}$ implies then that, when

$$\|\mathbf{y}\|_2 \geq \frac{2}{\sigma} \|\mathbf{H}_{x,y}f(x_0 + \alpha x, \mathbf{y}_0)\| \|\mathbf{x}\|_2,$$

we have

$$f(x_0 + \mathbf{x}, \mathbf{y}_0 + \mathbf{y}) \geq f(x_0 + \mathbf{x}, \mathbf{y}_0).$$

On the other hand, by the continuity of $\mathbf{H}f$, if we choose \mathbf{x} sufficiently small, then whenever

$$\|\mathbf{y}\|_2 \leq \frac{2}{\sigma} \|\mathbf{H}_{x,y}f(x_0 + \alpha x, \mathbf{y}_0)\| \|\mathbf{x}\|_2,$$

we have

$$\begin{aligned} \|\mathbf{H}_{x,y}f(x_0 + \alpha x, \mathbf{y}_0) \mathbf{H}_{y,y}f(x_0 + \mathbf{x}, \mathbf{y}_0 + \beta \mathbf{y})^{-1}\| &\leq \|\mathbf{H}_{x,y}f(x_0, \mathbf{y}_0) \mathbf{H}_{y,y}f(x_0, \mathbf{y}_0)^{-1}\| + \frac{1-\rho}{2} \\ &\leq \frac{1+\rho}{2} < 1 \end{aligned}$$

since f is ρ -forward biased. An application of Lemma 12 to Equation 8 with $\mathbf{B} = \mathbf{H}_{x,y}f(x_0 + \alpha x, \mathbf{y}_0)$ and $\mathbf{C} = \mathbf{H}_{y,y}f(x_0 + \mathbf{x}, \mathbf{y}_0 + \beta \mathbf{y})^{-1}$ then yields

$$f(x_0 + \mathbf{x}, \mathbf{y}_0 + \mathbf{y}) \geq f(x_0 + \mathbf{x}, \mathbf{y}_0).$$

whenever $\|\mathbf{y}\|_2 \geq \frac{1+\rho}{2} \|\mathbf{x}\|_2$. In other words,

$$\|g(x_0) - g(x_0 + \mathbf{x})\|_2 = \|\arg \min_{\mathbf{y}} f(x_0 + \mathbf{x}, \mathbf{y}_0 + \mathbf{y})\|_2 \leq \frac{1+\rho}{2} \|\mathbf{x}\|_2$$

so g is local radial $\frac{1+\rho}{2}$ -contractive, which is what was to be shown. \square

D.5 Myopic descent with tied weights

Theorem 13. *If $f(x, \mathbf{y}) : \mathbb{R}^a \times \mathbb{R}^a \rightarrow \mathbb{R}$ is forward-biased, σ -strongly convex, and L -smooth, then, for some step size $\eta > 0$, the iterates of myopic gradient descent with tied weights*

$$\mathbf{y}^{(t+1)} = \mathbf{y}^{(t)} - \eta \nabla_{\mathbf{y}} f(\mathbf{x}, \mathbf{y}^{(t)})|_{\mathbf{x}=\mathbf{y}^{(t)}}$$

converge to $\tilde{\mathbf{y}} \in \mathbb{R}^a$ satisfying

$$\tilde{\mathbf{y}} = \arg \min_{\mathbf{y} \in \mathbb{R}^a} f(\tilde{\mathbf{y}}, \mathbf{y}).$$

Proof. First, note that if myopic descent does converge, it must be to a point $\tilde{\mathbf{y}}$ such that $\tilde{\mathbf{y}} = \arg \min_{\mathbf{y}} f(\tilde{\mathbf{y}}, \mathbf{y})$. Indeed, at convergence we must have $\nabla_{\mathbf{y}} f(\tilde{\mathbf{y}}, \mathbf{y}) = 0$, so strong convexity tells us that $\tilde{\mathbf{y}}$ is optimal.

It remains only to establish that myopic descent converges to some $\tilde{\mathbf{y}}$, for small enough $\eta > 0$. It suffices to show that the gradient descent step

$$g_\eta(\mathbf{y}) = \mathbf{y} - \eta \nabla_{\mathbf{y}} f(\mathbf{x}, \mathbf{y})|_{\mathbf{x}=\mathbf{y}}$$

is contractive, and thus has a fixed point. Consider arbitrary \mathbf{y}_0 and \mathbf{y} . Then, by the mean value theorem,

$$\nabla_{\mathbf{y}} f(\mathbf{y}_0 + \mathbf{y}, \mathbf{y}_0 + \mathbf{y}) - \nabla_{\mathbf{y}} f(\mathbf{y}_0, \mathbf{y}_0) = (\mathbf{H}_{x,y}f(\mathbf{y}', \mathbf{y}') + \mathbf{H}_{y,y}f(\mathbf{y}', \mathbf{y}'))\mathbf{y} \quad (9)$$

for some $\mathbf{y}' \in [\mathbf{y}_0, \mathbf{y}_0 + \mathbf{y}]$. Furthermore,

$$\begin{aligned} \|g_\eta(\mathbf{y}_0 + \mathbf{y}) - g_\eta(\mathbf{y}_0)\|_2^2 &= \|\mathbf{y}_0 - \eta \nabla_{\mathbf{y}} f(\mathbf{y}_0, \mathbf{y}_0) - (\mathbf{y}_0 + \mathbf{y} - \eta \nabla_{\mathbf{y}} f(\mathbf{y}_0 + \mathbf{y}, \mathbf{y}_0 + \mathbf{y}))\|_2^2 \\ &= \|\mathbf{y}\|_2^2 + \eta^2 \|\nabla_{\mathbf{y}} f(\mathbf{y}_0, \mathbf{y}_0) - \nabla_{\mathbf{y}} f(\mathbf{y}_0 + \mathbf{y}, \mathbf{y}_0 + \mathbf{y})\|_2^2 \\ &\quad - 2\eta \langle \mathbf{y}, \nabla_{\mathbf{y}} f(\mathbf{y}_0, \mathbf{y}_0) - \nabla_{\mathbf{y}} f(\mathbf{y}_0 + \mathbf{y}, \mathbf{y}_0 + \mathbf{y}) \rangle. \end{aligned}$$

By Equation 9,

$$\langle \mathbf{y}, \nabla_{\mathbf{y}} f(\mathbf{y}_0, \mathbf{y}_0) - \nabla_{\mathbf{y}} f(\mathbf{y}_0 + \mathbf{y}, \mathbf{y}_0 + \mathbf{y}) \rangle = \mathbf{y}^\top (\mathbf{H}_{x,\mathbf{y}} f(\mathbf{y}', \mathbf{y}') + \mathbf{H}_{\mathbf{y},\mathbf{y}} f(\mathbf{y}', \mathbf{y}') \mathbf{y}) \quad (10)$$

$$\leq \|\mathbf{H}_{x,\mathbf{y}} f(\mathbf{y}', \mathbf{y}') \mathbf{H}_{\mathbf{y},\mathbf{y}} f(\mathbf{y}', \mathbf{y}')^{-1}\| \quad (11)$$

$$\leq \rho \|\mathbf{y}\|_2 \quad (12)$$

where (11) follows from Lemma 12, and (12) from ρ -forward bias. Hence, for small enough $\eta > 0$,

$$\|g_\eta(\mathbf{y}_0 + \mathbf{y}) - g_\eta(\mathbf{y}_0)\|_2^2 < m(\eta) \|\mathbf{y}\|_2$$

for some constant $m(\eta) < 1$ depending on η . We conclude that g is a contraction, as desired. \square

D.6 Properties of sine

Lemma 14. *Let $x \sim \mathcal{N}(0, 1)$. Then*

$$\text{Var}(\sin(bx)) = \frac{1}{2} - \frac{e^{-2b^2}}{2}.$$

Proof.

$$\text{Var}(\sin(bx)) = (2\pi)^{-1/2} \int_{-\infty}^{\infty} \sin^2(bx) e^{-x^2/2} dx = \frac{1}{2} - \frac{e^{-2b^2}}{2}.$$

\square

Lemma 15. *Let $x \sim \mathcal{N}(0, 1)$. Then*

$$\rho(x, \sin(bx)) = \frac{2be^{3b^2/2}}{e^{2b^2} - 1} \in O(e^{-b^2/2}),$$

where ρ is the Pearson correlation coefficient.

Proof. By symmetry, $\mathbb{E}[\sin(bx)] = 0$. We calculate

$$\text{Cov}(x, \sin(bx)) = (2\pi)^{-1/2} \int_{-\infty}^{\infty} x \sin(bx) e^{-x^2/2} dx = be^{-b^2/2}.$$

We already computed the variance in Lemma 14, so

$$\rho(x, \sin(bx)) = \frac{\text{Cov}(x, \sin(bx))}{\sqrt{\text{Var}(x)\text{Var}(\sin(bx))}} = \frac{2be^{3b^2/2}}{e^{2b^2} - 1}.$$

In our experiments we set $b = 10$, so $\rho(x, \sin(bx)) < 10^{-20}$.

E Model and training details: synthetic setting

We use a smaller version of the GPT-2 architecture, adapted to regression tasks. That is, the token embedding and unembedding layers are replaced with a trained linear map from the input space to the embedding space and from the embedding space to the output space, respectively. For each $p \in \{0.01, 0.1, 0.3, 1\}$ models are trained using ordinary and myopic descent on one epoch of 30 000 000 sequences of length 64 sampled from $\mathcal{D}_{p,10,10}^{64}$. See Table 3 for architecture details.

E.1 Probe details

Given a transformer model trained on \mathcal{D}_p , we sample the hidden states at each layer when the model is given as input 50 000 evaluation sequences from the same distribution \mathcal{D}_p . For each layer and targets $\sin(bx_{n-i})$ for varying $i > 0$, we fit a linear regression model on the hidden state of that layer to the target. The in-sample R^2 of each linear model is then reported.

Configuration Key	Value
num_layers	2
num_heads	2
embd_dim	128
n_inner	512
input_dim	2
output_dim	1
activation	relu
attn_pdrop	0
embd_pdrop	0
resid_pdrop	0
lr	1e-3
optimizer	AdamW
weight_decay	0.01
betas	(0.9, 0.99)
scheduler	cosine
warmup	0.01
batch_size	512
seq_length	64
loss_fn	HuberLoss

Table 3: Transformer configuration used when training on synthetic data distribution \mathcal{D}_p

F Model and training details: natural language setting

We train all models (vanilla and myopic) from random initialization for one epoch on 4.6M sequences from the MS MARCO dataset (Nguyen et al., 2016), truncated to length 64. To estimate the local myopia bonus of the vanilla model, we train another model from random initialization with the same architecture, but with past hidden states provided by the vanilla model; see Section C for details.⁹

G Future heads

The idea of the *future head* is to train a probe that takes (some subset of) the preceding hidden layers up to index t and the token sequence up to index $t + 1$ as input, and outputs a prediction of $G(x_{1:t+1})$. Since the future head is much simpler (in terms of number of parameters, training and inference compute consumed, etc.) than the full base model, nontrivial performance at this task could be interpreted as evidence of information in the hidden layers up to t that is useful to the prediction of not just token x_{t+1} , but also the following token x_{t+2} .

More precisely speaking, the future head is a model $f_\phi: \mathbb{R}^{d_{\text{hid}}tL} \times V^{t+1} \rightarrow \Delta^{|V|-1}$ such that for the full history of hidden states up to position t

$$h = (h_i^\ell(x)_{1:t} \mid 1 \leq i \leq t, 1 \leq \ell \leq L)$$

and the input sequence $x = x_{1:t+1}$, the future head’s output $f_\phi(h, x)$ is a prediction of the true base transformer output $G(x)$. However, although the entire hidden state trajectory h and input tokens x are fair game for the future head to take as input, they are in total fairly large; as mentioned above, we would like to keep the future head architecture simple. Thus, the architectures we consider limit the input to a small subset of the indices of h and x . Further, they only see the *embedded* tokens, borrowing the base transformer’s embedding E and unembedding D . For example, a natural setup to consider is taking as input only the

⁹Here, we do not use any existing pre-trained models (outside of the pre-trained tokenizer) for our experiments. This choice was made to avoid the interference of distribution shift and varying training schemes when comparing between the vanilla and myopic models.

Configuration Key	Value
num_layers	12
num_heads	12
embd_dim	768
n_inner	3072
vocab_size	50257
activation	gelu_new
attn_pdrop	0.1
embd_pdrop	0.1
resid_pdrop	0.1
lr	6e-4
optimizer	AdamW
weight_decay	0.01
betas	(0.9, 0.99)
scheduler	cosine
warmup	0.01
batch_size	512
seq_length	64
loss_fn	CrossEntropy

Table 4: Transformer configuration used when training on natural language data.

most recent last layer h_t^L and the most recent embedded token $E(x_{t+1})$. In this case, we can write f_ϕ as

$$f_\phi(h, x) = D(\hat{f}_\phi(h_t^L, E(x_{t+1})))$$

for a model $\hat{f}_\phi: \mathbb{R}^{d_{\text{hid}}} \times \mathbb{R}^{d_{\text{hid}}} \rightarrow \mathbb{R}^{d_{\text{hid}}}$, which we refer to as the *future neck*. More generally, for arbitrary subsets of indices $I \subseteq \{1, \dots, t\} \times \{1, \dots, L\}$ and $J \subseteq \{1, \dots, t+1\}$, using the convention that $h_I = (h_i^{i'} \mid (i, i') \in I)$ and $x_J = (x_j \mid j \in J)$, we can consider models of the form

$$f_\phi(h, x) = D(\hat{f}_\phi(h_I, E(x_J))).$$

In particular, when $I = \emptyset$, the future head does not consider the base model’s hidden state at all, and we are in the classical setting of predicting x_{t+1} from just (some subset of) the tokens $x_{1:t}$. We also train some simple models of this form for the purpose of comparison.

G.1 Loss definitions

For our purposes, the dataset consists of N sequences of exactly T tokens each:

$$X = \{(x_1^n, \dots, x_T^n)\}_{n=1}^N.$$

The base transformer is typically pre-trained using cross-entropy loss against the true next token:

$$\mathcal{L}_{\text{base}}(G_\theta; x) = \sum_{t=1}^{T-1} H(x_{t+1}^n, G_\theta(x_{1:t}^n)),$$

where we embed $x_{t+1} \in V \hookrightarrow \Delta^{|V|-1}$ in the natural way and we recall that H denotes the cross-entropy:

$$H(p, q) := - \sum_{i=1}^k p_i \log q_i$$

for discrete distributions $p, q \in \Delta^{k-1}$. In this setting, since the first argument is constant wrt. θ , this is equivalent to training on the Kullback-Leibler divergence:

$$D_{\text{KL}}(p \parallel q) := \sum_{i=1}^k p_i \log(p_i / q_i).$$

When training the future neck, we are interested in how closely its output on token x_t matches the base transformer’s output on token x_{t+1} , which is quantified by what we call the *self-prediction loss*, defined on a single sequence x by

$$\mathcal{L}_{\text{self}}(G_{\theta}, f_{\phi}; x) = \sum_{t=1}^{T-1} H(G_{\theta}(x_{1:t+1}), f_{\phi}(h(x_{1:t}), x_{1:t+1})).$$

As is standard, we then use a gradient-based method to approximate the solution to

$$\phi^* = \arg \min_{\phi} \mathcal{L}_{\text{self}}(G_{\theta}, f_{\phi}; X) = \arg \min_{\phi} \sum_{n=1}^N \mathcal{L}_{\text{self}}(G_{\theta}, f_{\phi}; x^n)$$

over the entire dataset X . It is also natural to consider the *future loss*:

$$\mathcal{L}_{\text{fut}}(G, f; x) = \sum_{t=1}^{T-2} H(x_{1:t+2}, f_{\phi}(h(x_{1:t}), x_{1:t+1})).$$

We might expect the future neck to have nontrivial performance on \mathcal{L}_{fut} simply because it is predicting $G(x_{1:t+1})$, which itself is a prediction of x_{t+2} .

G.2 Training the future head

We use the GPT-2 and Mistral-7B models for our future head experiments. For future necks that take as input only one or two of the preceding hidden states and input tokens, we use a linear architecture. For necks that consider the entire history, we use an LSTM. Note that a linear future neck that takes in as input only the embedded preceding token is equivalent to what we call an *embedded bigram* model in Section 5. Similarly, a future neck that takes no input whatsoever can only predict the mean, and is analogous to a unigram model.

Besides the losses explained in G.1, we also consider the following metrics used by (Din et al., 2023):

- Precision@ k : The proportion of data points in which the top probability token according to the future head is in the top- k tokens according to the base transformer.
- Surprisal: The negative log-probability, according to the base transformer, of the future head’s top probability token.

Our results are summarized in Table 5 and Table 6.

I_t	J_t	Probe	$\mathcal{L}_{\text{self}}$	\mathcal{L}_{fut}	Prec@1	Prec@10	Surprisal
\emptyset	\emptyset	Linear	7.918	7.759	0.051	0.371	3.317
\emptyset	$\{t+1\}$	Linear	6.076	5.852	0.263	0.604	2.332
\emptyset	$\{t, t+1\}$	Linear	5.79	5.56	0.303	0.662	2.225
\emptyset	$[2:t+1]$	LSTM	4.795	4.615	0.471	0.837	1.825
$\{t\} \times \{11\}$	\emptyset	Linear	6.403	5.276	0.237	0.486	2.254
$\{t\} \times \{11\}$	$\{t+1\}$	Linear	5.268	5.105	0.420	0.787	1.743
$\{t\} \times \{11\}$	$\{t, t+1\}$	Linear	5.201	5.033	0.428	0.794	1.798
$[1:t] \times \{11\}$	\emptyset	LSTM	5.693	5.54	0.325	0.570	2.202
$[1:t] \times \{11\}$	$[2:t+1]$	LSTM	4.564	4.414	0.539	0.887	1.700
$\{t\} \times \{12\}$	\emptyset	Linear	5.994	5.826	0.249	0.500	2.288
$\{t\} \times \{12\}$	$\{t+1\}$	Linear	4.921	4.729	0.441	0.804	1.833
$\{t\} \times \{12\}$	$\{t, t+1\}$	Linear	4.884	4.688	0.448	0.812	1.836
$[1:t] \times \{12\}$	\emptyset	LSTM	5.664	5.505	0.325	0.568	2.138
$[1:t] \times \{12\}$	$[2:t+2]$	LSTM	4.488	4.328	0.556	0.897	1.713

Table 5: Loss metrics for future heads on **GPT-2** given various combinations of inputs. For comparison, GPT-2 achieves next-token cross-entropy loss of **3.701**. Our convention is that, for example, $[1:t]$ denotes $\{1, \dots, t\}$. For Prec@ k higher is better, while for all other metrics lower is better.

I_t	J_t	Probe	$\mathcal{L}_{\text{self}}$	\mathcal{L}_{fut}	Prec@1	Prec@10	Surprisal
\emptyset	\emptyset	Linear	7.718	7.721	0.0364	0.2481	3.142
\emptyset	$\{t+1\}$	Linear	6.852	6.866	0.1616	0.5246	2.809
\emptyset	$\{t, t+1\}$	Linear	6.733	6.747	0.1731	0.516	2.734
\emptyset	$[2:t+1]$	LSTM	5.894	5.916	0.2244	0.5595	2.377
$\{t\} \times \{31\}$	\emptyset	Linear	4.629	4.658	0.3277	0.5654	1.856
$\{t\} \times \{31\}$	$\{t+1\}$	Linear	4.315	4.346	0.3970	0.6783	1.807
$\{t\} \times \{31\}$	$\{t, t+1\}$	Linear	4.317	4.384	0.3953	0.6766	1.808
$[1:t] \times \{31\}$	\emptyset	LSTM	4.427	4.460	0.3713	0.6039	1.741
$[1:t] \times \{31\}$	$[2:t+1]$	LSTM	3.813	3.850	0.4828	0.7176	1.55
$\{t\} \times \{32\}$	\emptyset	Linear	4.406	4.433	0.3387	0.5584	1.683
$\{t\} \times \{32\}$	$\{t+1\}$	Linear	4.083	4.112	0.4117	0.6745	1.605
$\{t\} \times \{32\}$	$\{t, t+1\}$	Linear	4.082	4.114	0.4106	0.6759	1.585
$[1:t] \times \{32\}$	\emptyset	LSTM	4.451	4.485	0.3648	0.6009	1.729
$[1:t] \times \{32\}$	$[2:t+1]$	LSTM	4.138	4.176	0.4214	0.6999	1.685

Table 6: Loss metrics for future heads on **Mistral-7B** given various combinations of inputs. For comparison, Mistral-7B achieves next-token cross-entropy loss of **2.238**.